Gastrointestinal defects of the *Gas1* mutant involve dysregulated Hedgehog and Ret signaling

Sandrine Biau[1,2,*], Shiying Jin[1,*] and Chen-Ming Fan[1,‡]

[1]Department of Embryology, Carnegie Institution of Washington, 3520 San Martin Drive, Baltimore, Maryland 21218, USA
[2]2iE Foundation, International Institute for Water and Environmental Engineering, Rue de la Science, 01 BP 594, Ouagadougou 01, Burkina Faso

*These authors contributed equally to this work
‡Author for correspondence (fan@ciwemb.edu)

Biology Open 2, 144–155
doi: 10.1242/bio.20123186
Received 24th September 2012
Accepted 2nd October 2012

Summary

The gastrointestinal (GI) tract defines the digestive system and is composed of the stomach, intestine and colon. Among the major cell types lining radially along the GI tract are the epithelium, mucosa, smooth muscles and enteric neurons. The Hedgehog (Hh) pathway has been implicated in directing various aspects of the developing GI tract, notably the mucosa and smooth muscle growth, and enteric neuron patterning, while the Ret signaling pathway is selectively required for enteric neuron migration, proliferation, and differentiation. The *growth arrest specific gene 1* (*Gas1*) encodes a GPI-anchored membrane protein known to bind to Sonic Hh (Shh), Indian Hh (Ihh), and Ret. However, its role in the GI tract has not been examined. Here we show that the *Gas1* mutant GI tract, compared to the control, is shorter, has thinner smooth muscles, and contains more enteric progenitors that are abnormally distributed. These phenotypes are similar to those of the *Shh* mutant, supporting that *Gas1* mediates most of the *Shh* activity in the GI tract. Because Gas1 has been shown to inhibit Ret signaling elicited by Glial cell line-derived neurotrophic factor (Gdnf), we explored whether *Gas1* mutant enteric neurons displayed any alteration of Ret signaling levels. Indeed, isolated mutant enteric progenitors not only showed increased levels of phospho-Ret and its downstream effectors, phospho-Akt and phospho-Erk, but also displayed altered responses to Gdnf and Shh. We therefore conclude that phenotypes observed in the *Gas1* mutant are due to a combination of reduced Hh signaling and increased Ret signaling.

Key words: Gas1, Gastrointestinal development, Ret, Shh

Introduction

The mammalian gastrointestinal (GI) tract is a complex digestive system. The entire tract develops from two ventral invaginations that fuse in the midline to form a straight gut tube in the gastrulating embryo. Subsequent morphogenic events divide the tube into distinct organs such as the stomach, intestine and colon. These organs have a similar radial organization: the endoderm-derived internal luminal epithelium, the splanchnic mesoderm-derived mucosa underneath the epithelium and smooth muscle layers (the circular and longitudinal) at the outer edge, and the neural crest-derived enteric neurons embedded in the mucosa and smooth muscles. The enteric neurons establish a mesh-work of innervations (collectively, the enteric nervous system or ENS) (reviewed by de Santa Barbara et al., 2003; Furness, 2006; Heanue and Pachnis, 2007) to control gut movement, digestive enzyme secretion, and nutrient absorption.

The gut endoderm expresses *Sonic hedgehog* (*Shh*) and *Indian hh* (*Ihh*) (Ramalho-Santos et al., 2000). Elimination of Hedgehog (Hh) signaling, by either removing the function of both *Shh* and *Ihh* or their obligatory signaling component *Smoothened* (*Smo*), leads to early lethality (Zhang et al., 2001). *Shh* single mutants develop further with a severely shortened GI tract, and a partial transformation of the stomach to intestine epithelium (Ramalho-Santos et al., 2000). *Ihh* mutants have defects in hindgut epithelium proliferation. Both *Shh* and *Ihh* single mutants also have thinner smooth muscle layers, indicating that they stimulate smooth muscle proliferation. Importantly, conditional inactivation of *Shh* and *Ihh* via Shh^{Cre} revealed their critical role in gut mesoderm expansion (Mao et al., 2010). Mice mutant for *Gli2* or *Gli3*, both downstream mediators of Hh signaling, also display GI tract defects similar to, albeit milder than, that of the *Shh* mutant (Mo et al., 2001; Kim et al., 2005). *Shh* mutants have an apparent increase in ectopic localized enteric neurons whereas a fraction of *Ihh* mutants has virtually no enteric neurons (Ramalho-Santos et al., 2000), suggesting their opposing roles in enteric neuron development. As the primary effect of Hh signal is in the mesenchyme, whether the documented enteric phenotypes result from a direct action of Hh is uncertain. For example, Hh signaling was reported not active in the enteric neurons between the smooth muscle layers, i.e. the myenteric plexus, based on the expression of its downstream reporters, *Ptc1-LacZ* and *Gli1-LacZ* (Kolterud et al., 2009). On the other hand, endogenous Ptc1 expression was detected in the myenteric plexus (Fu et al., 2004). In addition, the recombinant N-terminal fragment of the active portion of Shh (Shh-N) can stimulate proliferation of enteric progenitors, which is in agreement with *Ihh* mutant phenotype but contrast with the apparent *Shh* mutant phenotype (Fu et al., 2004). Thus, how Hh signaling controls enteric neuron development along the GI tract remains elusive.

The majority of the neurons in the ENS originate from the enteric neural crest (ENC) at the vagal level (reviewed by Burns, 2005; Heanue and Pachnis, 2007; Newgreen and Young, 2002; Taraviras and Pachnis, 1999). They migrate to reach the rostral end of the intestine and enter the mesodermal layer, in which they migrate rostrocaudally and circumferentially along the GI tract, continuing to proliferate while they migrate and to differentiate into a variety of neuronal subtypes (Furness, 2006). The migration and colonization of the ENCs depends on Glial-derived neurotrophic factor (Gdnf) expressed in the gut mesenchyme (Golden et al., 1999; Natarajan et al., 2002). Gdnf appears to act as a chemoattractant to guide ENCs (Asai et al., 2006; Natarajan et al., 2002; Yan et al., 2004; Young et al., 2001). Consistently, the ENCs express Gdnf receptor-α1 (Gfrα1) (Chalazonitis et al., 1998; Worley et al., 2000) and the receptor tyrosine kinase Ret (Taraviras et al., 1999): the former binds to Gdnf and couples to the latter for signal transduction. This signaling axis is also critical to enteric neuron progenitor survival, proliferation, and differentiation (Gianino et al., 2003) and involves downstream effectors such as Akt and Erk (Asai et al., 2006; Hayashi et al., 2000; Mograbi et al., 2001; reviewed by Airaksinen and Saarma, 2002). Importantly, mice mutant for *Gdnf*, *Gfrα1*, or *Ret*, lack enteric neurons in the small and large intestine (Enomoto et al., 1998; Jain et al., 2004; Moore et al., 1996; Pichel et al., 1996; Sánchez et al., 1996; Schuchardt et al., 1994; Tomac et al., 1999). Of clinical relevance, lack of enteric neurons in segments of the intestine causes congenital intestinal obstruction in humans known as the Hirschsprung's disease (HSCR) (Brooks et al., 2005; Gershon and Ratcliffe, 2004).

Enteric neuron progenitors in the GI tract can be isolated and cultured as enteric neurospheres (Bondurand et al., 2003). Shh-N and Gdnf have been shown to counteract each other's activity in such a culture system. Shh enhances enteric progenitor proliferation, whereas Gdnf promotes differentiation (Fu et al., 2004). Such observation, coupled with *Shh* and *Ihh* expression in the epithelium and *Gdnf* in the mesenchyme, supports a notion that they coordinately control enteric progenitor and neuron numbers via long-range versus local actions. Recent data revealed that Growth arrest-specific gene 1 (Gas1) is both a Hh and a Ret binding protein (Cabrera et al., 2006; Lee et al., 2001a), suggesting that it can play a role in coordinating these two pathways. Although Gas1 was thought to be an unique membrane protein without homologs (Schneider et al., 1988), advanced computational studies re-assigned it to be a member of the Gfrα family (Cabrera et al., 2006; Schueler-Furman et al., 2006). For the Hh pathway, Gas1 appears to act as a co-receptor by facilitating Hh binding to its receptor Ptc1, which then results in canonical pathway activation (Martinelli and Fan, 2007a). For the Ret pathway, over-expressed Gas1 was shown to suppress Gdnf-induced tyrosine phosphorylation of Ret at Y1062 (López-Ramírez et al., 2008), as well as phosphorylation of its downstream effector Akt in cell lines (Cabrera et al., 2006; López-Ramírez et al., 2008). While the involvement of Gas1 in Hh signaling is well established *in vitro* and *in vivo*, the role of Gas1 in modulating Ret signaling has not been investigated beyond these initial *in vitro* studies.

To explore the possibility that Gas1 integrates Shh and Ret signaling *in vivo*, we first established that *Gas1* is expressed in the developing GI tract. We found that *Gas1* mutant GI tract has circular smooth muscle defects that can be attributed to defective Hh signaling. The abnormality of enteric progenitor organization and proliferation found in *Gas1* mutants is more likely explained by a combination of reduced Hh signaling and increased Ret signaling. We further utilized the enteric neurosphere cultures derived from *Gas1* control and mutant embryonic GI tracts to delineate the contribution of Shh and Ret in the proliferation and differentiation of enteric progenitors. Our results have implications to other organs and cell types where both Hh and Ret signaling pathways are active.

Materials and Methods

Generation of embryos

Gas1^{LacZ} (Martinelli and Fan, 2007a) and *Shh* (Chiang et al., 1996) mutant alleles were described previously. Heterozygous mating was used to generate mutant embryos of desired genotypes (determined by PCR reactions) and specific stages described in the text. The vaginal plug date is designated as embryonic day 0.5 (E0.5) following convention. All procedures are approved by Carnegie IACUC.

Histology, histochemistry, and immunostaining

For histology, embryos younger than E13.5 or dissected GI tracts (for embryos older than E13.5) were fixed in Methacarn, dehydrated in methanol, embedded in paraffin, sectioned, and stained by hematoxylin and eosin (Surgipath). For X-gal reaction and immunofluorescence, embryos or GI tracts were fixed in 4% paraformaldyhyde/PBS for 2 hrs, extensively washed in PBS, transferred through serial sucrose/PBS, and embedded in OCT for cryosectioning. Primary antibodies used were: anti-β-gal (rabbit, Chemicon, 1:1000, or mouse, Promega, 1:1000), anti-smooth muscle actin (SMA, rabbit, Abcam, 1:200), anti-neural-specific β-tubulin (Tuj1, mouse, Covance, 1:800), anti-Neurotrophin receptor p75 (Rabbit, Millipore, 1:200), 1:200, Ret (goat, R&D system, 1:100), and anti-mouse Gas1 (goat, R&D system, 1:200). Alexa fluor 488 and Alexa fluor 568 conjugated secondary antibodies against specific species (goat, mouse, and rabbit) were used for detection (Molecular Probes, all at 1:1000). DAPI was used at 1 μg/ml for counter staining of DNA.

In situ hybridization (ISH)

Freshly dissected guts were fixed in Methancarn, dehydrated in methanol, embedded in paraffin, and sectioned. ISH was performed using a standard protocol (Schaeren-Wiemers and Gerfin-Moser, 1993) with digoxygenin-labeled antisense RNA probes. The *Shh* probe was a gift from Dr A. McMahon (Harvard University), the *Ptc1* probe, a gift from Dr M. Scott (Stanford University).

RT-PCR

For each sample, 1 μg of total RNA was used for standard reverse transcription (RT) using random primers and MMLV reverse transcriptase (Invitrogen) in a 15 μl reaction. One μl of the RT reaction was then used in a 20 μl Polymerase Chain Reaction (PCR) for 30–35 cycles. The oligonucleotide primers used for each are as follows. *Gdnf*: GAAGTTATGGGATGTCGTGGC and CGTAGCCCAA-ACCCAAGTCAG; *Shh*: GAAGATCACAAGAAACTCCGAACG and TGGATT-CATAGTAGACCCAGTCGAA; *Gli1*: ATCACCTGTTGGGGATGCTGGAT and GGCGTGAATAGGACTTCCGACAG; Actin: TGGGAATGGGTCAGAAGG-ACT and GGGTCATCTTTTCACGGTTGGC. Products were resolved on 2% agarose gels and presented as qualitative assessments.

Neurosphere culture

Neurosphere-like bodies were generated with E11.5 whole guts of specified genotypes as previously described (Bondurand et al., 2003; Fu et al., 2004). 10 nM of Shh-N (Martinelli and Fan, 2007a) or 50 ng/ml of GDNF (recombinant human GDNF, Peprotech) were used in culture as specified in text and legends. Neurospheres cultures were fixed and stained as previously described (Fu et al., 2004) using antibodies described above.

Proliferation assay

For *in vivo* labeling, EdU (5 μg/gram of body weight) in PBS was injected into the pregnant mice peritoneally, and the embryos were harvested 1 hr later. For *in vitro* labeling, EdU (0.5 μg/ml) was added 1 hr before the termination of culture. EdU detection was performed using the Click-iT kit (Invitrogen) after immunostaining procedure.

Western blots

Control and mutant neurospheres were incubated in serum-free medium for 4 h and then mock-stimulated or stimulated with 10 nM of Shh-N or 50 ng/ml of Gdnf in serum free medium for 10 min. Approximately 20–30 neurospheres were used per condition. They were lysed in ice-cold RIPA buffer supplemented with protease inhibitor, phosphatase inhibitors and 1 mM PMSF (Promega). Nuclei

were removed by centrifugation, 4× SDS-PAGE sample buffer was added, and samples were resolved by 7.5% SDS-PAGE. Western blots were performed using rabbit antibodies against Akt, phospho-Akt (P-Akt), Erk1/2 (collectively, Erk), phospho-Erk1/2 (collectively, P-Erk), Ret, and phospho-Ret-Y1062 (P-Ret; Cell Signaling) followed by HRP-conjugated secondary antibody and ECL detection (Amersham). Band intensities were quantified using densitometry, followed by Image J program. At least 3 independent experiments were performed for each condition for statistical evaluation.

Quantitation and statistical analyses

Circular smooth muscle thickness was measured based on anti-SMA staining. $P75^{+}$ and EdU^{+} cells were counted on digital images of ≥5 sections of each of ≥3 embryos of each genotype. Bar graphs represent mean ± standard deviations. All statistical data considered significant were with P values <0.05 as assessed by the Student's t-test; t-test was performed for paired samples, and ANOVA with Tukey *post hoc* corrections performed for paired and multiple comparisons. They are presented in text or legends as appropriate.

Results

Gas1 is expressed in the developing mouse GI tract

As the first step towards investigating *Gas1* function in the developing GI tract, we examined its expression. Using a *LacZ* knock-in allele of *Gas1* ($Gas1^{LacZ}$) (Martinelli and Fan, 2007a), we monitored β-gal activity (by X-gal histochemical reaction) as a reporter for *Gas1* expression in $Gas1^{+/LacZ}$ embryos. At E8.5, β-gal positive cells were found at the dorsal gut endoderm and the splanchnic mesoderm (Fig. 1A). At the E9.5 midgut level, the dorsal endoderm staining was preferentially localized to the left side and the splanchnic mesoderm staining becomes more intensified (Fig. 1B). The significance for such asymmetric expression is currently unknown. At E11.5, X-gal staining was detected in the gut mesenchyme (Fig. 1C), but no longer in the endodermal epithelium of the stomach and midgut. From E13.5 to E15.5 and E18.5 (Fig. 1D–L), staining in the mesenchyme between the epithelium and smooth muscles becomes progressively reduced, and eventually staining is only seen in the two smooth muscle layers. Similar changes were found in the stomach (Fig. 1D,G,J), intestine (Fig. 1E,H,K) and colon (Fig. 1F,I,L). At E13.5 and E15.5, we noted some cells lightly stained with variable intensities scattered in between the smooth muscle layers, i.e. the myenteric plexus. The latter suggests that enteric progenitors or neurons express *Gas1*. At E18.5, X-gal staining was detected intensely throughout the two muscle layers as well as cells between them in the stomach and small intestine, while much weaker or no X-gal signal was found in cells in the myenteric plexus of the colon. *Gas1* expression in the smooth muscles suggests a role in mediating Hh signaling for the growth of these muscles, while expression in myenteric plexus suggests a role in mediating Hh and/or Ret signaling for enteric progenitor/neuron development.

Gas1 mutant mice have multiple morphological GI tract defects

To assess the function of *Gas1* in GI development, we examined the phenotype of *Gas1* mutants. Although *Gas1*-LacZ expression in the GI system is detected early, we did not find appreciable defects in the gut tube at E10.5 and E11.5. However, at postnatal day 0, the mutant GI tract was ~60% the length of the control GI tract, while the mutant embryo weighed at 75–80% of the control sibling. However, the mutant stomach was ~1/4 the size of the control stomach, indicating a disproportional deficiency in the growth of this organ. The mutant gut also displayed slight malrotation (Fig. 2A).

Because most *Gas1* mutants died immediately after birth and were cannibalized, we focused our analysis at E18.5, one day

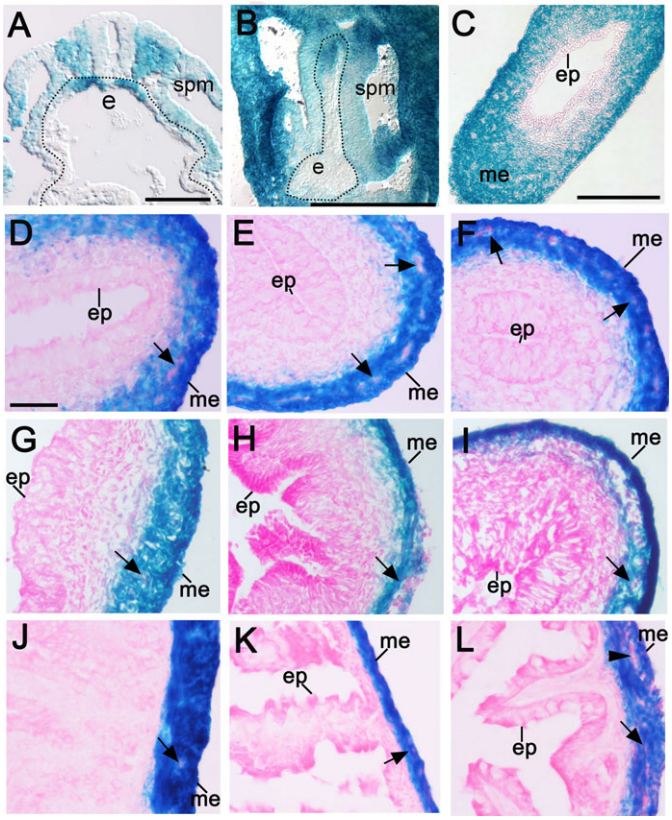

Fig. 1. *Gas1* is expressed in the developing gut. *Gas1-LacZ* pattern is determined by X-gal reactions on sections of $Gas1^{+/LacZ}$ embryos and GI tracts. (**A**) At E8.5, the signal is detected in the dorsal endoderm (e, outlined) and the splanchnic mesoderm (spm). (**B**) At E9.5, the signal is still in the spm and asymmetrically in the endoderm. (**C**) At E11.5, the blue signal is in mesoderm (me) but not in epithelium (ep). (**D–L**) Persistent staining is found in the mesoderm of the stomach (D,G,J), midgut (E,H,K), and hindgut (F,I,L) at E13.5 (D–F), E15.5 (G–I) and E18.5 (J–L). At E13.5 and E15.5, scattered cells in the submucosa distant from the epithelium are positive, and weakly positive cells are found between the mesodermal layers, presumably the progenitors/neurons of the myenteric plexus (arrows). At E18.5, the entire circular and longitudinal muscles and the myenteric plexus are positive, while the hindgut myenteric plexus displays weakly positive and negative cells (arrowhead). Scale bars: 0.5 mm in A,B; 0.25 mm in C; 50 μm in D–L.

prior to birth. The *Gas1* mutant not only had a much smaller stomach, but also displayed an overgrown stomach epithelium by histological analysis (compare Fig. 2B and Fig. 2C), a phenotype previously reported for the *Shh* mutant (Fig. 2D) (Ramalho-Santos et al., 2000). Although *Shh* mutant has a partial stomach-to-midgut transformation, as its epithelium is positive for Alkaline Phosphatase activity (specific for midgut) (Ramalho-Santos et al., 2000), such transformation is not found in the *Gas1* mutant (not shown). *Gas1* mutants also displayed occlusion by overgrown villi (compare Fig. 2E and Fig. 2F), which is reminiscent of the duodenal stenosis (Gray and Skandalakis, 1972; Riddlesberger, 1989) and is a phenotype also described for the *Shh* mutant (Fig. 2G) (Ramalho-Santos et al., 2000). We confirmed that *Shh* mutants had imperforate anus, i.e. the colon terminates in a blind dilation not fused to the surface ectoderm. *Gas1* mutants did not have this defect. The muscle wall of the colon in either *Gas1* or *Shh* mutants was visibly thinner than the control (Fig. 2H–J). Thus, consistent with previously conclusions for the neural tube, craniofacial structures, somite, and limb defects (Martinelli and

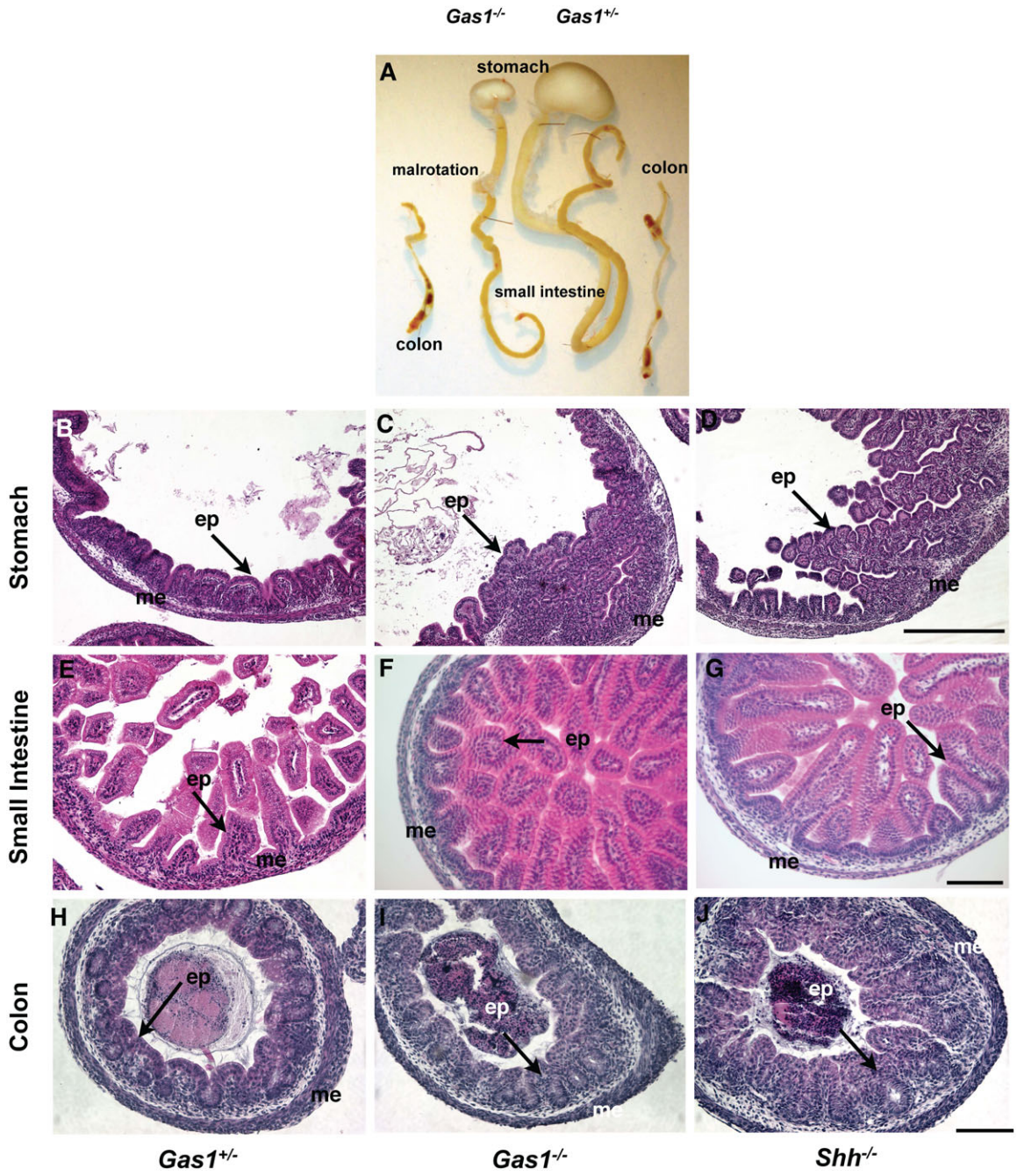

Fig. 2. *Gas1* mutant GI tract has morphological defects. (**A**) Whole mount gastrointestinal tracts of $Gas1^{-/-}$ and $Gas1^{+/-}$ embryos: the left GI tract is from $Gas1^{-/-}$ embryo, and the right one from $Gas1^{+/-}$ embryo, at P0. The stomach, small intestine, and colon are labeled. The overall length of the mutant GI tract is ~60% of the control tract. Mutant stomach size is only ~1/4 of the control. Also, the mutant displays slight malrotation between the duodenum and the small intestine. Hematoxylin and Eosin stained histological sections of $Gas1^{+/-}$ (**B**,**E**,**H**), $Gas1^{-/-}$ (**C**,**F**,**I**) and $Shh^{-/-}$ (**D**,**G**,**J**) GI tracts at E18.5. In the stomach, the $Gas1^{-/-}$ (C) and the $Shh^{-/-}$ (D) display an overgrown stomach epithelium compared to $Gas1^{+/-}$ (B). In the small intestine, the $Gas1^{-/-}$ (F) and the $Shh^{-/-}$ (G) display an occlusion by overgrown villi compare to the $Gas1^{+/-}$ (E). (H–J) Cross-sections of $Gas1^{+/-}$ (H), $Gas1^{-/-}$ (I), and $Shh^{-/-}$ (J) colons. Scale bars: 0.5 mm in B–D; 0.1 mm in E–J.

Fan, 2007a), the *Gas1* mutant displays milder defects than those found in the *Shh* mutant, including the GI tact.

Gas1 mutants display circular smooth muscle defects

Both *Shh* and *Ihh* single mutants were reported to have reduced circular smooth muscle thickness. To determine whether endogenous Gas1 is expressed in the circular smooth muscles to mediate their function, we performed double immunofluorescence with anti-Gas1 and anti-SMA antibodies. We found that their expression overlapped in both circular and longitudinal smooth muscle layers (Fig. 3A–C), consistent with the X-gal histochemical data.

While we confirmed the circular muscle defects in the *Shh* mutant (Fig. 3F), we did not find such a defect in the *Ihh* mutant

(not shown; see Discussion). Using smooth muscle actin (SMA) as a marker for the muscle layers, we found that *Gas1* mutants, like *Shh* mutants, had thinner circular smooth muscle layer in the small intestine, compared to the control (Fig. 3D–F). We further quantified the circular muscle thickness of *Shh* and *Gas1* mutants in the stomach, small intestine, and colon. In comparison to $Gas1^{+/LacZ}$, which is similar to wild type controls, *Gas1* and *Shh* mutants respectively showed 27% and 33% reduction in stomach circular muscle layer (Fig. 3G), 58% and 33% reduction in the small intestine circular muscle layer (Fig. 3H), and 40% and 62.6% in colon circular muscle layer (Fig. 3I). Although the longitudinal smooth muscles appeared disorganized in both *Gas1* and *Shh* mutants, their thickness was relatively normal. The differential severities of *Gas1* versus *Shh* mutants at different levels of the GI tract may be due to differential expression and/or compensation by other Hh pathway components. These data together support that Hh released from the epithelium can reach the circular muscle layer (Kolterud et al., 2009; Ramalho-Santos et al., 2000), where Gas1 helps to enhance the signaling output.

Gas1 mutants have reduced Hh signaling

If Gas1 indeed mediates Hh signaling in the gut, we expect to find reduced expression of Hh signal transcriptional targets, such as *Ptc1*, in the *Gas1* mutant. At E11.5, *Shh* was expressed normally in the mutant epithelium (compare Fig. 4A and Fig. 4B), whereas occasional patches of the mutant mesenchyme showed reduced *Ptc1* (compare Fig. 4C and Fig. 4D), suggesting not an overt reduction of Hh signaling at this point. At E15.5, reduced *Ptc1* expression in the intestine (Fig. 4G,H) and colon (Fig. 4K,L) was evident: only the mesenchyme immediately adjacent to the epithelium expressed elevated levels of *Ptc1* in the mutant, while the control showed the up-regulated *Ptc1* expression domain extending further into the surrounding mesenchyme and apparently in the circular muscle layer. Although *Shh* expression in the mutant small intestine appeared normal, its expression in the mutant colon was visibly reduced (Fig. 4E,F,I,J). On the other hand, *Ihh* expression levels did not appear qualitative different between control and mutant small intestines and colons (supplementary material Fig. S1). As *Gas1* is not expressed in the epithelium after E11.5, these data indicate a feedback regulation from defective smooth muscles (or other cell types) in the *Gas1* mutant to down-regulate *Shh* expression in the colon epithelium. The reduced range and level of *Ptc1* expression likely reflect the lack of *Gas1* to extend Shh's range of action in the small intestine. In the colon, however, *Ptc1* reduction may be attributed to the reduction of *Shh* and loss of *Gas1*. Nevertheless, the complementary expression pattern of *Shh* in the secretion site and *Gas1* in the receiving site supports them as a ligand-receptor pair. We note that the endocrine secreting CCK+ cells in the mutant duodenum

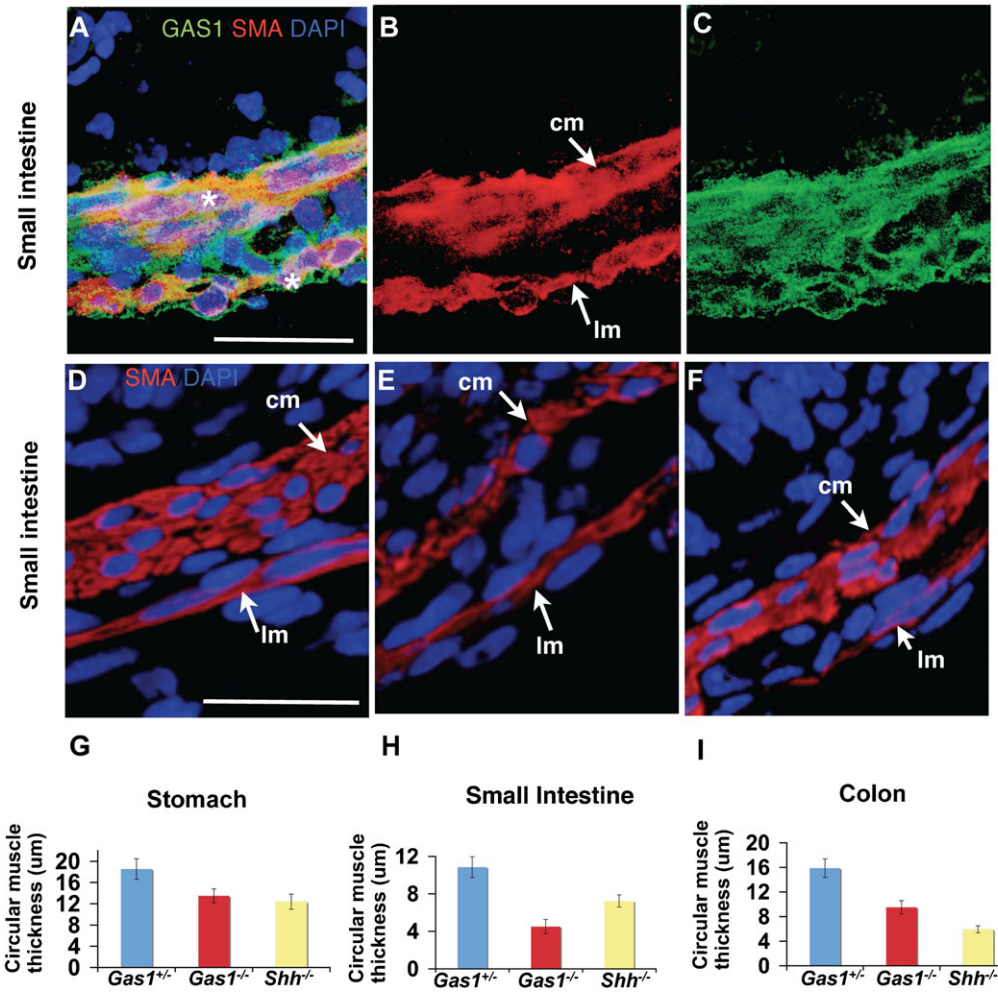

Fig. 3. *Gas1* mutants have a thinner circular smooth muscle layer similar to that of *Shh* mutants. (**A–C**) In E18.5 wild type small intestine, endogenous Gas1 (C) and SMA (B) expression overlaps (A, with DAPI) in both layers of smooth muscles; asterisks in (A) indicate the overlap; cm, circular smooth muscle; lm, longitudinal muscle. (**D–F**) Circular smooth muscle defects are shown for small intestines of $Gas1^{-/-}$ (E) and $Shh^{-/-}$ (F) at E18.5, compared to the $Gas1^{+/-}$ control (D); longitudinal muscle (lm) layers are slightly disorganized in both mutants. The thickness of the circular smooth muscle layers in $Gas1^{+/-}$, $Gas1^{-/-}$ and $Shh^{-/-}$ is quantified in μm (mean; error bars = standard deviation) for stomach (**G**), small intestine (**H**), and colon (**I**). For $Gas1^{+/-}$ stomach, 18.5±1.9; small intestine, 10.85±1.1; and colon, 15.9±1.5. For $Gas1^{-/-}$ stomach, 13.5±1.3; small intestine, 4.51±0.76; and colon, 9.5±1.09. For $Shh^{-/-}$ stomach, 12.4±1.4; small intestine, 7.23±0.65; and colon, 5.9±0.56. In stomach, small intestine and colon, $Gas1^{-/-}$ has 27.3%, 58.4% and 40.3% reduction, and $Shh^{-/-}$ has 33.2%, 30.6% and 62.5% reduction, respectively, compared to $Gas1^{+/-}$. Scale bars: 25 μm in A (also applies to B,C) and in D (also applies to E,F).

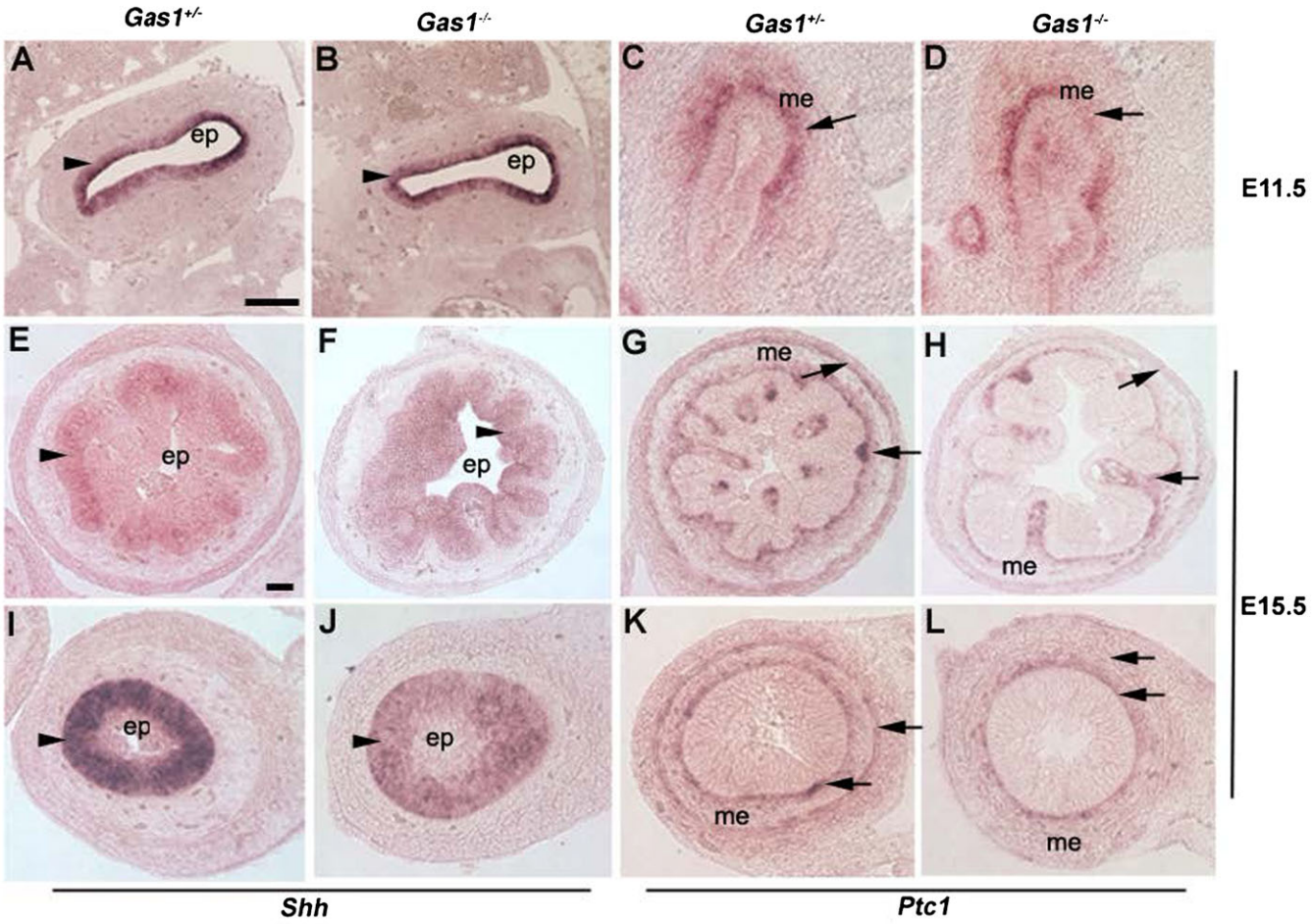

Fig. 4. Hh signaling is altered in the *Gas1* mutant GI tract. At E11.5, the *Gas1*$^{-/-}$ (**B**,**D**) does not have an altered expression of *Shh* in the endoderm epithelium (ep), but a slightly reduced level of *Ptc1* in patches of the mesenchyme (me) at stomach level compared to the control (**A**,**C**). At E15.5 small intestine level, the *Gas1*$^{-/-}$ (**F**) has a similar level of *Shh* expression in the epithelium as the control (**E**). *Ptc1* expression is reduced in the submucosa and nearly absent at the circular muscle layer (**H**). In the colon, *Shh* expression level is reduced in the *Gas1* mutant (**J**) compare to the control (**I**), and *Ptc1* expression is restricted to the mesenchyme immediately below the epithelium in the *Gas1* mutant (**L**), compared to the control (**K**). Arrows point to signals in the mesenchyme, the mucosa immediately underneath the epithelium, and the outer layer, presumably the circular smooth muscle; arrowheads in epithelium. Scale bars: 100 μm in A (also applies to B–D), and in E (also applies to F–L).

epithelium are present, implying not an overt change in the *Gas1* mutant epithelium patterning (supplementary material Fig. S2).

Gas1 mutants have altered enteric progenitor number and distribution

Shh mutants were described to have substantial enteric neurons, suggesting that it inhibits enteric progenitor proliferation (Ramalho-Santos et al., 2000). We therefore examined whether *Gas1* mutants have a similar change in enteric neurons to that found in *Shh* mutants.

At E18.5, the control myenteric neurons formed coalesced clusters between the two muscle layers (stained by Tuj1) (supplementary material Fig. S2). The *Gas1* mutant had abundant enteric neurons that were scattered and disorganized, and some were mis-localized to near the base of the epithelium. This patterning defect was also documented for the *Shh* mutant (Ramalho-Santos et al., 2000). As Tuj1 and GFAP positive cells were found abundantly in the mutant (supplementary material Fig. S2), there appeared no major defects in the terminal differentiation of neurons and glia *per se*. Because Shh is implicated in enteric progenitor proliferation (Fu et al., 2004), we next examined whether endogenous Gas1 is expressed in the enteric progenitors using P75 as a marker. Indeed, we observed P75^{+} enteric progenitors in the small intestine stained positively for endogenous Gas1 antigen (Fig. 5A–C). Importantly, in the small intestine, there were approximately 1.6-fold more P75^{+} progenitors per cross section at E18.5 in the *Gas1* mutant than in the control (Fig. 5D,E, and quantification in Fig. 5F). Furthermore, the mutant P75^{+} cells were less organized and some of them were found ectopically located near the epithelium (Fig. 5E). To determine whether the increase in enteric progenitors in the mutant is due to increased proliferation, we monitored their proliferation rate at E13.5, an earlier time-point when the enteric progenitors actively expand. At this time-point, the mutant P75^{+} progenitors appeared normally distributed (Fig. 5H). *In vivo* EdU incorporation assay revealed that among the P75^{+} cells, P75^{+}EdU^{+} cells were found at a 2-fold higher rate in the *Gas1* mutant than in the control (Fig. 5G,H, and quantification in Fig. 5I). Thus, the *Gas1* mutant displays similar enteric neural defects to that described for the *Shh* mutant.

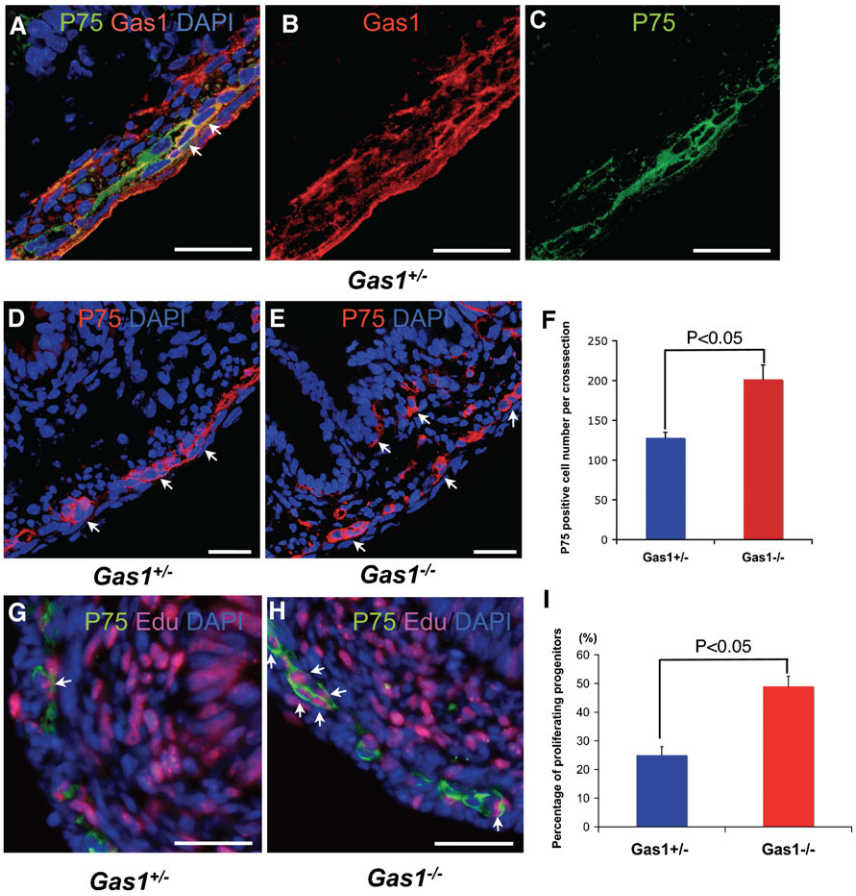

Fig. 5. The enteric nervous system is defective in the *Gas1* mutant. Immunofluorescence of E18.5 small intestine transverse sections for P75 (**C**), endogenous Gas1 (**B**), and their overlaid image with DAPI (**A**) counterstaining shows that Gas1 is expressed in the enteric progenitors/neurons. (**D–F**) At E18.5, compared to the *Gas1* heterozygotes ($Gas1^{+/-}$; D), the *Gas1* mutant ($Gas1^{-/-}$; E) displayed more enteric progenitors/neurons at a per section basis; quantification in (F): 128±8 *vs* 201±18 ($P<0.05$) and mutant cells were also found at ectopic locations in the mesenchyme. (**G–I**) The increased proliferation rate of *Gas1* mutant enteric progenitors was found as early as in the E13.5 small intestine. EdU incorporation was used to monitor proliferating cells. The percentages of $p75^{+}$ cells with EdU signal in controls and mutants are quantified in (I): 25±3% *vs* 49±4% ($P<0.05$), from 3 embryos and ≥100 $P75^{+}$ cells per embryo counted. Color codes for each staining agents are as indicated. Arrows point to cells with positive signals. Scale bars: 25 μm in A–E,G,H.

The *Gas1* mutant small intestine has altered levels of phosphorylated Akt and phosphorylated Erk

Because Gas1 was suggested to inhibit Ret signaling by *in vitro* cell line assays (Cabrera et al., 2006; López-Ramírez et al., 2008), we wanted to determine whether the defect observed in *Gas1* mutant enteric system is associated with elevated Ret signaling. Despite multiple attempts, we failed to reliably detect phosphorylated Ret using anti-phospho-Ret-Y1062 (P-Ret), a phosphorylation event critical for Ret signaling (Jain et al., 2006; Jijiwa et al., 2004; Wong et al., 2005), on small intestine sections or tissue extracts by Western blot. However, we were able to detect phosphorylation of Ret downstream effectors, Akt (P-Akt) and Erk (P-Erk), in extracts. After normalization to total Akt and Erk, both P-Akt and P-Erk levels were consistently found to be slightly increased in the *Gas1* mutant compared to the control (supplementary material Fig. S3) intestine. Although this change is consistent with increased Ret signaling, a plethora of signaling pathways converging to Akt and Erk and multiplicity of cells types in the intestine preclude us to make a firm conclusion that these detected changes are due to changes of the enteric population and Ret signaling.

Gas1 mutant cells possess the ability to form neurospheres, but are compromised in mediating canonical Hh signaling

To remove the complexity of cell types existed in the whole GI tract and to delineate the potential contribution of Gas1 in modulating Hh versus Ret signaling in the enteric system, we utilized the enteric neurosphere assay. Importantly, the antagonistic activities of Shh-N and Gdnf were documented using E11.5 derived neurospheres (Fu et al., 2004).

We noted that primary $Gas1^{-/-}$ neurospheres initially formed more abundantly but smaller than $Gas1^{+/-}$ control neurospheres in a reproducible manner (Fig. 6A,B). X-gal reactions on these spheres revealed that the *Gas1* promoter remained active during the culturing condition for both control and mutant. After secondary expansion, the mutant cells gave rise to neurospheres in efficiency and of size ranges similar to those of control cells. In order to have sufficient neurospheres of similar sizes for assay, subsequent experiments used neurospheres after secondary expansion and derived from multiple independent control and mutant embryos.

Double immunofluorescence for β-gal and Ret of $Gas1^{+/LacZ}$ enteric neurospheres showed that neurospheres contained many $\beta\text{-gal}^{+}\text{Ret}^{+}$ cells (Fig. 6C–E), legitimizing the use of this system to assess the role of *Gas1* in modulating Ret signaling. Control and mutant neurospheres established by this method expressed minimal levels of *Gdnf* or *Shh* transcripts by RT-PCR compared to E11.5 gut tubes of corresponding genotypes (Fig. 6F), making them suitable for determining the consequences of exogenously applied factors. Consistently, neither control nor mutant neurospheres expressed detectable levels of the Hh downstream gene *Gli1* without exogenously applied Shh-N. To confirm that these neurospheres were responsive to Hh signaling, we applied recombinant Shh-N at 10 nM (previously determined to induce sub-maximal response) (Martinelli and Fan, 2007a) for 24 hrs and assayed for the induction of *Gli1*. We found that mutant neurosheres were qualitatively less responsive than control neurospheres (Fig. 6G), suggesting the positive role of Gas1 in facilitating Hh signaling in this system, as in other tissues reported previously (Martinelli and Fan, 2007a).

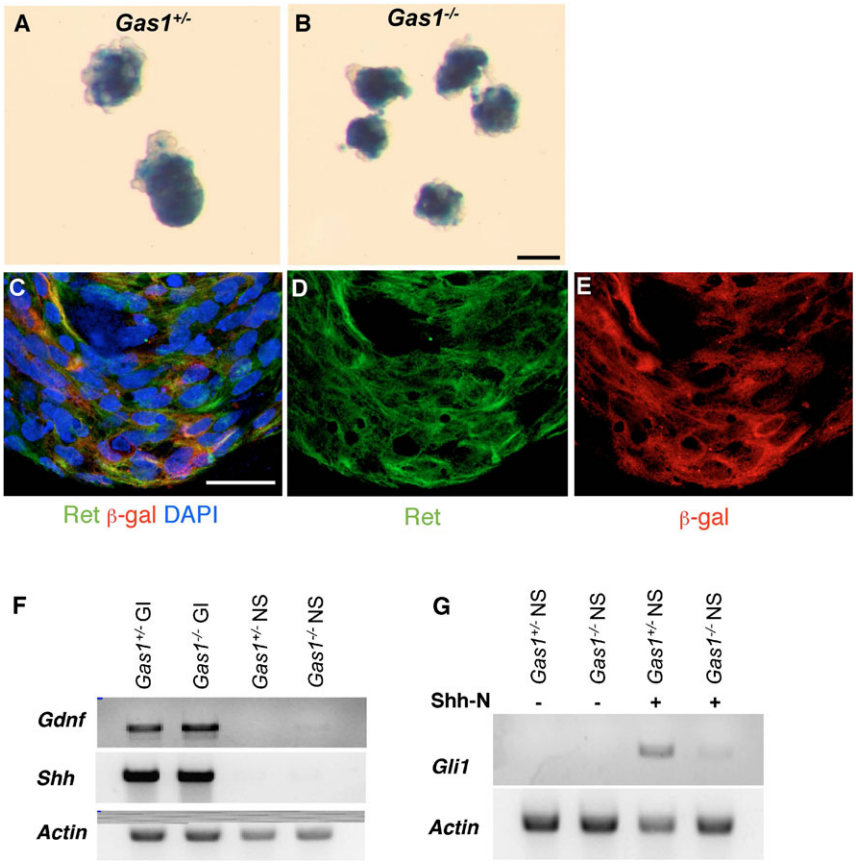

Fig. 6. *Gas1* mutant enteric neurospheres are less responsive to exogenously applied Shh-N. Primary *Gas1* control ($Gas1^{+/-}$) (**A**) and mutant ($Gas1^{-/-}$) (**B**) enteric neurospheres were subjected to X-gal reaction. (**C–E**) Single plane confocal image of the control enteric neurosphere stained for anti-Ret (D) and anti-β-gal (E), combined with DAPI (C). Note that in (A–E), not all cells in enteric neurospheres were positive for X-gal or β-gal. (**F**) RT-PCR for *Gdnf*, *Shh*, and *β-actin* (*Actin*) transcripts using E11.5 control and mutant GI tracts (GI), as well as enteric neurospheres derived from the respective genotypes. (**G**) RT-PCR for *Gli1* and *β-actin* expression in control and mutant neurospheres, either mock-treated (−) or treated with 10 nM of Shh-N (+) for 24 hrs. Scale bars: 0.2 mm in A,B; 25 μm in C–E.

Gas1 modulates Ret and its downstream effectors

We next wanted to test whether there was an alteration of Ret signaling in the *Gas1* mutant neurosphere, because Gas1 was suggested to impact Gdnf-induced Ret signaling (Cabrera et al., 2006; López-Ramírez et al., 2008). We also monitored two effectors that have been implicated to mediate Ret-regulated cell proliferation and differentiation, i.e. Akt and Erk (Airaksinen and Saarma, 2002; Asai et al., 2006; Hayashi et al., 2000; Mograbi et al., 2001). For signaling levels, Western analysis was performed using antibodies to Y1062 phosphorylated Ret (P-Ret), P-Erk and P-Akt. Total Ret, Erk and Akt levels were also monitored to determine relative ratios of their respective phosphorylated forms. For optimization of monitoring above phosphorylation events, we varied the dosages of Shh-N (10–40 nM) and Gdnf (0.75–100 ng/ml), and conducted time-course studies (5–20 min, at 5 min intervals). Consistent with previous reports, we found that 10 nM Shh-N and 50 ng/ml of Gdnf are at sub-maximal for response (Fu et al., 2004; Martinelli and Fan, 2007a), and that 10 min after Gdnf and Shh-N application resulted in the most robust effect. Below, we describe data from these conditions.

We were first surprised to find that after switching to the basal medium without addition of Gdnf or Shh-N, *Gas1* mutant neurospheres reproducibly displayed an increased level of P-Ret (Fig. 7) than that in the control neurospheres (1.56 fold, $P=0.014$). Similarly, P-Erk (2.02 fold, $P=0.012$) and P-Akt (1.98 fold, $P=0.003$) levels are also increased in the mutant neurospheres. After acute application of Gdnf for 10 min, both control and mutant neurospheres were stimulated to display significantly increased levels of P-Ret as well as P-Akt and P-Erk, compared to untreated control ($0.0007 \leq P \leq 0.016$ for all). *Gas1* mutant neurospheres treated with Gdnf showed further increased levels of P-Ret ($P=0.079$), P-Erk ($P=0.018$), and P-Akt ($P=0.047$) compared to the mutant untreated sample.

Unexpectedly, we found that acutely applied Shh-N (10 min) also stimulated P-Erk (2.89 fold, $P=0.023$) and P-Akt (2.17 fold, $P=0.004$) in control neurospheres (compared to untreated), without significantly inducing P-Ret as with Gdnf. These data indicate that Shh-N pulse elicits Erk and Akt pathway activation in enteric neurospheres. Although Shh-N appeared to increase P-Erk and P-Akt levels in the mutant neurosphere relative to mutant untreated sample, but the increases were not significant (for P-Erk, 2.24 *vs* 2.02 fold, $P=0.15$; for P-Akt, 1.98 *vs* 1.72 fold, $P=0.13$). These results together indicate that removal of *Gas1* function in enteric neurospheres makes them spuriously activate Ret signaling, and become less responsive to Shh-N-induced P-Erk and P-Akt activation, as well as *Gli1* expression (Fig. 6G). Thus, we have uncovered Akt and Erk as potential Gas1-modulated nodal points of crosstalk between Hh and Ret signaling.

Gas1 mutant neurospheres have altered response to Shh-N and Gdnf

The above data prompted us to investigate whether the biochemical alterations observed in the *Gas1* mutant neurosphere had any significance in functional alteration. It was established that the enteric neurosphere system allowed detection of Shh-N-induced proliferation and Gdnf-induced neuronal differentiation (Fu et al., 2004) – despite Gdnf-Ret signaling is also known to stimulate enteric progenitor proliferation (Gianino et al., 2003; Hearn et al., 1998;

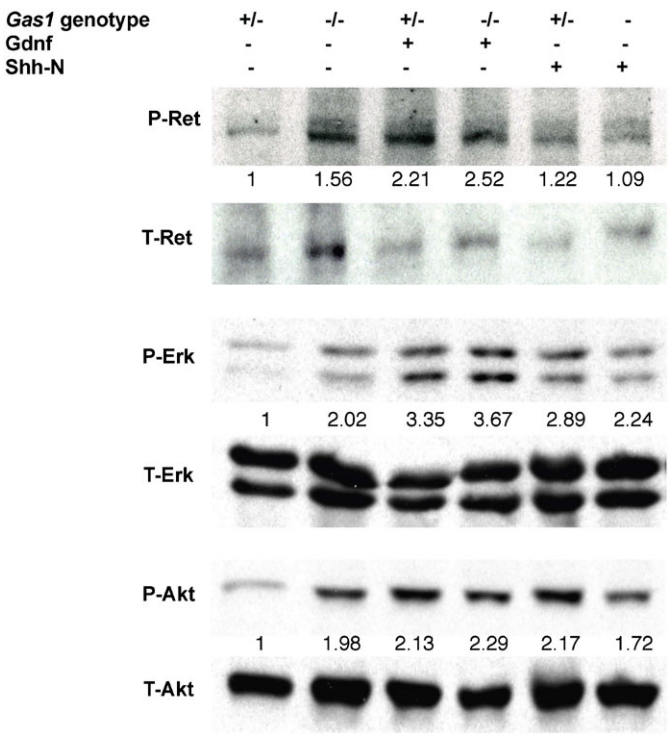

Fig. 7. *Gas1* mutant neurospheres have altered levels of P-Ret, P-Akt, and P-Erk. $Gas1^{+/-}$ and $Gas1^{-/-}$ neurospheres were cultured in serum free medium for 4 hrs, then mock-treated or treated with Gdnf or Shh-N (in serum free medium) for 10 min. Cell lysates were subjected to Western analysis using anti P-Ret, anti-P-Erk and anti-P-Akt antibodies. Total Ret (T-Ret), Erk (T-Erk) and Akt (T-Akt) levels were separately probed using the same amount from each sample for controls to determine the ratios of their respective phosphorylated forms by densitometry. Densitometry was done using exposures with non-saturated signal intensities. The data shown are a set of representative examples from 3 independent experiments. The quantification presented is the average fold difference relative to control mock-treated samples and is indicated below the phosphorylated epitopes. Standard deviations are omitted, and those of statistical significance based on various paired comparisons (see Materials and Methods) are specifically stipulated in the text with *p* values stated.

Heuckeroth et al., 1998). To study their effects, we cultured the control and mutant neurospheres in the absence or presence of recombinant Shh-N or Gdnf. We used EdU incorporation to monitor proliferation (Fig. 8A–F) and Tuj1 immunostaining to monitor neuronal differentiation (Fig. 8G–L).

Consistent with previous report (Fu et al., 2004), we found that exogenous Shh-N increased the proliferation rate of the control neurosphere relative to that of the untreated sample (Fig. 8A,B, and quantification in Fig. 8M). *Gas1* mutant neurospheres also responded to applied Shh-N, but to a lesser extent (Fig. 8D,E,M). By contrast, when Gdnf was used to stimulate proliferation, EdU incorporation rate was increased but no significant differences between control and mutant neurospheres were obtained (Fig. 8C,F,M). When Tuj1 was used for assaying neuronal differentiation, we noted that Shh-N did not enhance enteric neuron differentiation in control and mutant, compared to the untreated condition (Fig. 8G,H,J,K, and quantification in Fig. 8N). Gdnf, on the hand, effectively enhanced neuronal differentiation of the control neurospheres, and this effect was further increased in the *Gas1* mutant (Fig. 8I,L, and quantification in Fig. 8N). Thus, removal of *Gas1* leads to blunted Shh-N response in proliferation and elevated Gdnf response in differentiation. Below we discuss the ramification of our findings.

Discussion

The role of Hh signaling in gastrointestinal development has been firmly established (Kim et al., 2005; Litingtung et al., 1998; Mao et al., 2010; Ramalho-Santos et al., 2000). Such a role has been shown in the zebrafish GI tract (Reichenbach et al., 2008). Here we extend this observation by describing the role of the Hh binding protein Gas1. We further provide evidence that *Gas1* mutant enteric neurospheres display elevated levels of Ret signaling as well as its downstream effectors. It appears that Gas1 has diverged from the core Gfrα family to acquire Hh binding and signaling capacity, while gaining constitutive Ret binding property in an inhibitory manner, to effect enteric neuron development.

Gas1 and Hh signaling

We have previously shown that *Gas1* mutants display many phenotypes related to the *Shh* mutant, albeit to a lesser degree (Martinelli and Fan, 2007a; Martinelli and Fan, 2007b). In the Hh signaling cascade Gas1 is placed parallel to the Hh receptor Ptc1. Gas1 and Ptc1 together display a greater Shh-N binding activity than either one alone, but the precise biophysical nature for this synergy is not known. Here, we show that inactivation of the *Gas1* gene alone is sufficient to cause GI defects related to reduced Hh signaling, including reduced GI tract length, malrotation of the gut, reduced circular muscle thickness, overgrowth of the villi, and hyper abundance of enteric neurons. Aspects of *Gas1* mutant GI defects are more severe than those of the *Shh* mutant, while other aspects milder. The more severe phenotypes, e.g. circular smooth muscle thickness at the midgut, may be due to *Gas1* also mediating Ihh signaling. However, the *Ihh* allele in our mouse colony did not render GI defects reported for the *Ihh* mutant (Ramalho-Santos et al., 2000) – likely due to different genetic backgrounds used. We note that the circular smooth muscles of $Shh^{+/-}Gas1^{-/-}$ and $Ihh^{+/-}Gas1^{-/-}$ midgut were not statistically thinner than that of $Gas1^{-/-}$ midgut (not shown), suggesting that *Gas1* mutation is dominant to produce the phenotype and precludes observable genetic interaction with *Shh* and *Ihh* in their heterozygous backgrounds. This perhaps explains the more severe phenotype in the *Gas1* mutant than in the *Shh* mutant in this context. The milder phenotypes, e.g. the GI tract length, may be explained by the compensation by *Cdo* and/or *Boc*, two additional Hh binding proteins. Recent studies have shown that Cdo and Boc play a redundant role with Gas1 to mediate Hh signaling at various tissues examined (Allen et al., 2011; Allen et al., 2007). Notably, the *Gas1;Cdo;Boc* triple mutant is similar to the *Smo* mutant (i.e. a complete loss of Hh signaling) (Allen et al., 2011; Zhang et al., 2001). The precise contribution of each to the GI tract needs extensive future studies. It is also important to keep in mind that Gas1, Cdo, and Boc have functions seemingly unrelated to Hh signaling (Lee et al., 2001b; Liu et al., 2002; Lu and Krauss, 2010; Wegorzewska et al., 2003).

Because *Gas1* is expressed in the circular smooth muscle, we propose that it directly mediates the reception of Hh secreted from the epithelium for growth. Indeed, expression of *Hh* signaling reporters indicates that Hh signaling is active in the gut mesenchyme and circular muscle (Kolterud et al., 2009). Furthermore, *Shh-Cre* driven conditional *Ihh;Shh* mutant has a

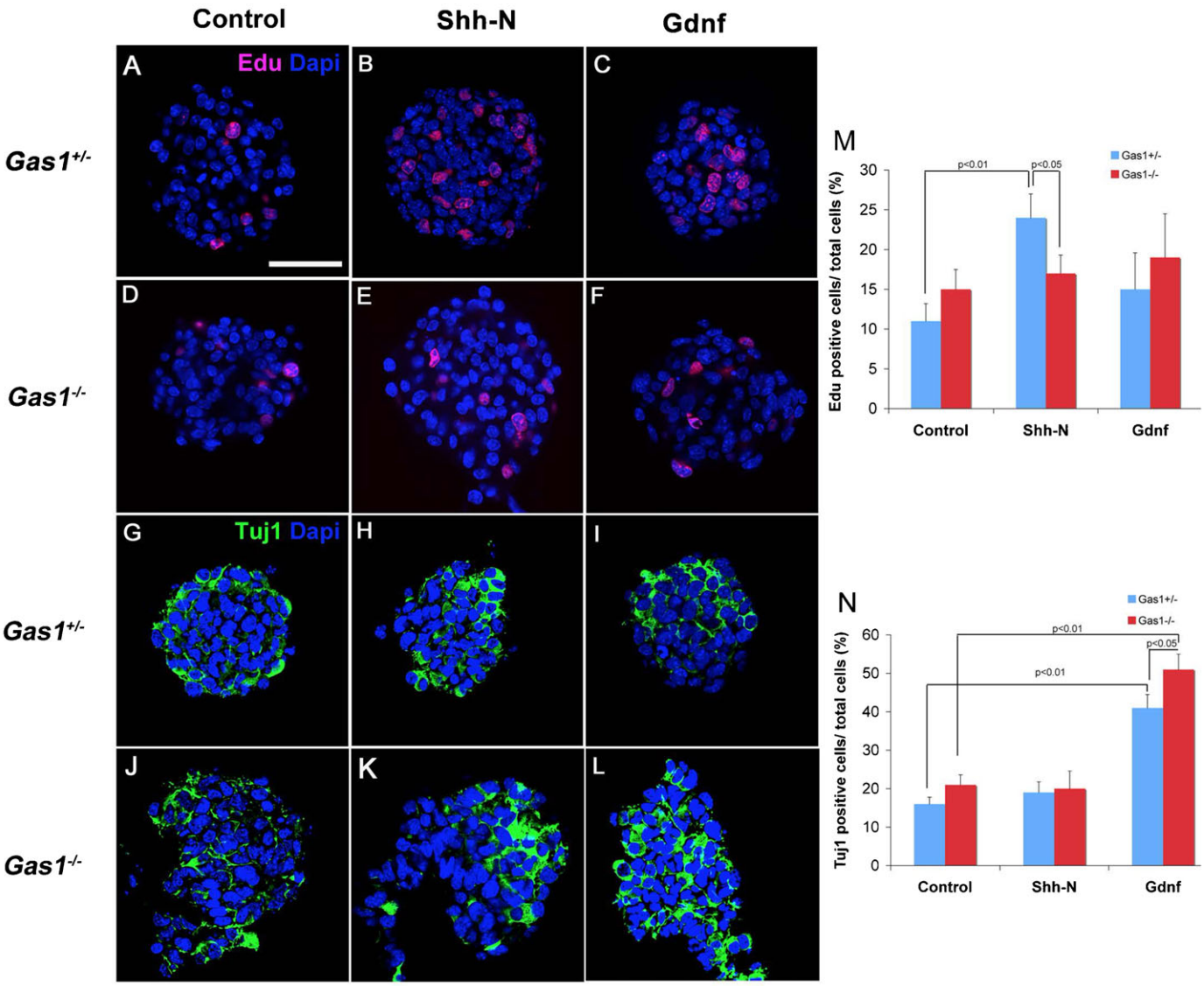

Fig. 8. Shh-N and Gdnf exert differential effects on *Gas1* mutant neurospheres. *Gas1*$^{+/-}$ (**A–C,G–I**) and *Gas1*$^{-/-}$ (**D–F,J–L**) neurospheres were mock-treated (control; A,D,G,J), treated with 10 nM Shh-N (B,E,H,K) or treated with 50 ng/ml Gdnf (C,F,I,L). EdU was added one hour before harvesting. Controls were performed in side-by-side experiments (A,D,G,J). Proliferation was detected by EdU (red) incorporation (A–F), while neuronal differentiation was detected by Tuj1 (green) immunostaining (G–L). All neurospheres were countered staining with DAPI (blue). Scale bar: 0.1 mm in A–L. (**M**) Quantification of proliferation: compared to the mock-treated, *Gas1*$^{+/-}$ neurospheres treated with Shh-N displayed higher rate of proliferation (11±2% *vs* 24±3%, $P<0.01$). *Gas1*$^{-/-}$ neurospheres were less responsive to Shh-N than *Gas1*$^{+/-}$ neurospheres (17±2% *vs* 24±3%, $P<0.05$). No significant differences were found for Gdnf treatment. (**N**) Quantification of differentiation: for both *Gas1*$^{+/-}$ and *Gas1*$^{-/-}$ neurospheres, Gdnf stimulated significant differentiation related to control mock-treated ($P<0.01$ for both). *Gas1*$^{-/-}$ neurospheres were more responsive to Gdnf than *Gas1*$^{+/-}$ neurospheres (51±3% *vs* 41±3%, $P<0.05$).

drastic reduction of gut mesenchyme and smooth muscles, and expression of an activated *Smo* (Smo-M2) drastically increases mesenchymal mass (Mao et al., 2010). Mice mutant for the transcriptional mediators of Hh signaling, *Gli2* or *Gli3*, also display GI defects similar to that of the *Shh* mutant (Mo et al., 2001; Kim et al., 2005). Lastly, transgenic expression of *Ihh* via a *Villin* promoter causes overt villus smooth muscle differentiation (Kolterud et al., 2009). All these results support the role of Hh signaling in the expansion of embryonic gut mesoderm.

Transient expression of *Gas1* in the dorsal endoderm is similarly to that of *Ptc1-LacZ* (Kolterud et al., 2009). Their early expression suggests autocrine signaling in the endoderm and may help explain the GI malrotation phenotype shared by *Shh* and *Gas1* mutants. Since *Gas1* is not detected in the villi, villi overgrowth in the mutant likely reflects a secondary consequence. Whether myenteric progenitors and neurons receive Hh signaling *in vivo* remain unresolved by different downstream reporter studies (Fu et al., 2004; Kolterud et al., 2009). Functional studies also generated puzzling results. In the zebrafish, Hh signaling appears essential for enteric progenitor migration/proliferation via mutational and pharmacological assays (Reichenbach et al., 2008). In the mouse, however, inactivating both *Shh* and *Ihh* in the endoderm did not lead to a deficiency of enteric neurons (Mao et al., 2010), whereas overexpression of *GLI1* (presumably activating Hh signaling) causes patchy absence of enteric neurons along the GI tract

(Yang et al., 1997). Our X-gal expression survey indicated that *Gas1*^{LacZ} expression in the myenteric layer is dynamic. Importantly, we show that endogenous Gas1 co-localizes with P75^{+} progenitors, suggesting that they do have the potential to receive Hh signal. The disorganization and ectopic localization of enteric progenitors/neurons found in both *Shh* and *Gas1* mutants also support that reduced Hh signaling can cause radial patterning/cell-positioning defects in the gut (Ramalho-Santos et al., 2000). Shh-N can promotes enteric progenitor proliferation in neurosphere culture (Fu et al., 2004) and we show that *Gas1* potentiates such *in vitro* activity. However, both the *Shh* mutant and *Gas1* mutant GI tracts contain abundant enteric progenitor/neurons. Thus, while Hh signaling may influence enteric neuron pool size *in vivo*, this role appears more modulatory than essential. Instead, the increased rate of P75^{+} progenitor proliferation found in the *Gas1* mutant intestine indicates a negative role of Gas1, likely linked to suppressing Ret signaling.

Gas1 and Ret signaling

Gas1 and Ret were shown to interact with each other by co-immunoprecipitation in cell lines (Cabrera et al., 2006). Over-expressed Gas1 was shown not to alter Gdnf-Gfrα1-Ret complex formation (Cabrera et al., 2006) and it reduced the activation of their downstream effector Akt (Cabrera et al., 2006; López-Ramírez et al., 2008). Our neurosphere data reveal a role for Gas1 in suppressing the spurious activation of both effectors, presumably via suppressing the basal activity of Ret. Because Ret signaling is known to mediate cell proliferation and survival via various signaling branches, including Erk and Akt (Airaksinen and Saarma, 2002; Asai et al., 2006; Hayashi et al., 2000; Mograbi et al., 2001), the increased proliferation of *Gas1* mutant enteric progenitors may be associated with elevated Ret signaling. Although the culture condition used to maintain the enteric progenitor state is only permissive for assaying Gdnf-mediated differentiation activity (Elia et al., 2007; Fu et al., 2004), *Gas1* mutant cells did show enhanced response to Gdnf. Given the importance of Ret and Gdnf in the expansion of enteric progenitor pool (Gianino et al., 2003; Hearn et al., 1998; Heuckeroth et al., 1998), and the increase in P-Ret, P-Erk, and P-Akt, and enhanced response to Gdnf of *Gas1* mutant neurospheres, we propose that increased Ret signaling level is a candidate mechanism underlying the increased proliferative rate observed in *Gas1* mutant enteric progenitors.

Gas1-Shh versus Gas1-Ret

We have tested the four core members of the Gfrα family (Gfrα1–4) and found that they all lack Shh-N binding activity in a COS cell surface binding assay (not shown). Thus, Gas1 is a unique member of this family to acquire Hh binding activity. Gas1 has no identifiable homolog in *Drosophila* in which the Hh signaling pathway is extensively studied. How it has evolved to play a substantial role in mediating Hh signaling in the mouse is an intriguing question. It is equally intriguing that Gas1 has also evolved to gain the Gdnf-independent Ret binding capacity but adopts an inhibitory role, while the core Gfrα members need engagement of specific Gdnf-related ligands for Ret binding and activation. How Gas1 becomes co-evolved to integrate these two signaling pathways or accidentally evolved to modulate them independently in different contexts will require investigation of species with an identifiable Gas1 gene and active Hh and Ret signaling pathways.

Here we show that Gas1 impinges on Hh and Ret signaling levels. Not only is Gas1 needed to suppress P-Ret, P-Erk and P-Akt levels, it is also needed for maximal P-Akt and P-Erk induction by Shh-N. We suggest that the proliferative effect of Shh-N is mediated by its canonical pathway, while the immediate Erk and Akt activation reflects its cooperation with other signaling pathways. In myoblast cultures Shh-N has also been shown to activate Akt and Erk and cooperate with IGF-1, which signals through a receptor tyrosine kinase (Elia et al., 2007; Madhala-Levy et al., 2012). Cellular levels of activated Akt and Erk conversely impact canonical Hh signaling (Riobo et al., 2006a; Riobó et al., 2006b). In enteric progenitors and myoblasts, we presume P-Erk and P-Akt activation by Hh potentiates receptor tyrosine kinase signaling. We imagine that the integration between Hh and Ret via Gas1 is extended to other contexts as a general regulatory theme.

Further defining the physical interfaces of Gas1-Shh and Gas1-Ret binding should allow the design of function distinguishing mutations of Gas1. For example, a missense mutation in *GAS1* associated with holoprosencephaly was recently characterized as deficient for Shh-N binding (Pineda-Alvarez et al., 2012). It is possible that this mutated GAS1 retains Ret binding property. Conversely, based on the modeled interactions between Ret and Gfrαs (Cabrera et al., 2006; Schueler-Furman et al., 2006), a mutation in Gas1 may be engineered to selectively disrupt Ret but not Hh binding. Exclusive binding mutations of Gas1 for Shh and Ret will be the key future tools to resolve Gas1's contribution to each pathway.

Acknowledgements

We thank all members of the Fan lab for helpful discussions and manuscript reading. We also thank Mr Evan Siple for genotyping, and Mr Blake Weber, Ms Rebecca Obniski, and Ms Yue Zheng for their technical assistance during their rotations. This work is supported by Carnegie endowment and an NIH grant to C.-M.F. (RO1 DK084963).

Competing Interests

The authors have no competing interests to declare.

References

Airaksinen, M. S. and Saarma, M. (2002). The GDNF family: signalling, biological functions and therapeutic value. *Nat. Rev. Neurosci.* **3**, 383-394.

Allen, B. L., Tenzen, T. and McMahon, A. P. (2007). The Hedgehog-binding proteins Gas1 and Cdo cooperate to positively regulate Shh signaling during mouse development. *Genes Dev.* **21**, 1244-1257.

Allen, B. L., Song, J. Y., Izzi, L., Althaus, I. W., Kang, J. S., Charron, F., Krauss, R. S. and McMahon, A. P. (2011). Overlapping roles and collective requirement for the coreceptors GAS1, CDO, and BOC in SHH pathway function. *Dev. Cell* **20**, 775-787.

Asai, N., Fukuda, T., Wu, Z., Enomoto, A., Pachnis, V., Takahashi, M. and Costantini, F. (2006). Targeted mutation of serine 697 in the *Ret* tyrosine kinase causes migration defect of enteric neural crest cells. *Development* **133**, 4507-4516.

Bondurand, N., Natarajan, D., Thapar, N., Atkins, C. and Pachnis, V. (2003). Neuron and glia generating progenitors of the mammalian enteric nervous system isolated from foetal and postnatal gut cultures. *Development* **130**, 6387-6400.

Brooks, A. S., Oostra, B. A. and Hofstra, R. M. (2005). Studying the genetics of Hirschsprung's disease: unraveling an oligogenic disorder. *Clin. Genet.* **67**, 6-14.

Burns, A. J. (2005). Migration of neural crest-derived enteric nervous system precursor cells to and within the gastrointestinal tract. *Int. J. Dev. Biol.* **49**, 143-150.

Cabrera, J. R., Sanchez-Pulido, L., Rojas, A. M., Valencia, A., Mañes, S., Naranjo, J. R. and Mellström, B. (2006). Gas1 is related to the glial cell-derived neurotrophic factor family receptors α and regulates Ret signaling. *J. Biol. Chem.* **281**, 14330-14339.

Chalazonitis, A., Rothman, T. P., Chen, J. and Gershon, M. D. (1998). Age-dependent differences in the effects of GDNF and NT-3 on the development of neurons and glia from neural crest-derived precursors immunoselected from the fetal rat gut: expression of GFRα-1 *in vitro* and *in vivo*. *Dev. Biol.* **204**, 385-406.

Chiang, C., Litingtung, Y., Lee, E., Young, K. E., Corden, J. L., Westphal, H. and Beachy, P. A. (1996). Cyclopia and defective axial patterning in mice lacking *Sonic hedgehog* gene function. *Nature* **383**, 407-413.

de Santa Barbara, P., van den Brink, G. R. and Roberts, D. J. (2003). Development and differentiation of the intestinal epithelium. *Cell. Mol. Life Sci.* **60**, 1322-1332.
Elia, D., Madhala, D., Ardon, E., Reshef, R. and Halevy, O. (2007). Sonic hedgehog promotes proliferation and differentiation of adult muscle cells: Involvement of MAPK/ERK and PI3K/Akt pathways. *Biochim. Biophys. Acta* **1773**, 1438-1446.
Enomoto, H., Araki, T., Jackman, A., Heuckeroth, R. O., Snider, W. D., Johnson, E. M., Jr and Milbrandt, J. (1998). GFRα1-deficient mice have deficits in the enteric nervous system and kidneys. *Neuron* **21**, 317-324.
Fu, M., Lui, V. C., Sham, M. H., Pachnis, V. and Tam, P. K. (2004). Sonic hedgehog regulates the proliferation, differentiation, and migration of enteric neural crest cells in gut. *J. Cell Biol.* **166**, 673-684.
Furness, J. B. (2006). *The Enteric Nervous System*. Malden, MA: Blackwell Publishing.
Gershon, M. D. and Ratcliffe, E. M. (2004). Developmental biology of the enteric nervous system: pathogenesis of Hirschsprung's disease and other congenital dysmotilities. *Semin. Pediatr. Surg.* **13**, 224-235.
Gianino, S., Grider, J. R., Cresswell, J., Enomoto, H. and Heuckeroth, R. O. (2003). GDNF availability determines enteric neuron number by controlling precursor proliferation. *Development* **130**, 2187-2198.
Golden, J. P., DeMaro, J. A., Osborne, P. A., Milbrandt, J. and Johnson, E. M., Jr. (1999). Expression of neurturin, GDNF, and GDNF family-receptor mRNA in the developing and mature mouse. *Exp. Neurol.* **158**, 504-528.
Gray, S. W. and Skandalakis, J. E. (1972). *Embryology For Surgeons: The Embryological Basis For The Treatment Of Congenital Defects*. Philadelphia: Saunders.
Hayashi, H., Ichihara, M., Iwashita, T., Murakami, H., Shimono, Y., Kawai, K., Kurokawa, K., Murakumo, Y., Imai, T., Funahashi, H. et al. (2000). Characterization of intracellular signals via tyrosine 1062 in RET activated by glial cell line-derived neurotrophic factor. *Oncogene* **19**, 4469-4475.
Heanue, T. A. and Pachnis, V. (2007). Enteric nervous system development and Hirschsprung's disease: advances in genetic and stem cell studies. *Nat. Rev. Neurosci.* **8**, 466-479.
Hearn, C. J., Murphy, M. and Newgreen, D. (1998). GDNF and ET-3 differentially modulate the numbers of avian enteric neural crest cells and enteric neurons *in vitro*. *Dev. Biol.* **197**, 93-105.
Heuckeroth, R. O., Lampe, P. A., Johnson, E. M. and Milbrandt, J. (1998). Neurturin and GDNF promote proliferation and survival of enteric neuron and glial progenitors *in vitro*. *Dev. Biol.* **200**, 116-129.
Jain, S., Naughton, C. K., Yang, M., Strickland, A., Vij, K., Encinas, M., Golden, J., Gupta, A., Heuckeroth, R., Johnson, E. M., Jr et al. (2004). Mice expressing a dominant-negative Ret mutation phenocopy human Hirschsprung disease and delineate a direct role of Ret in spermatogenesis. *Development* **131**, 5503-5513.
Jain, S., Encinas, M., Johnson, E. M., Jr and Milbrandt, J. (2006). Critical and distinct roles for key RET tyrosine docking sites in renal development. *Genes Dev.* **20**, 321-333.
Jijiwa, M., Fukuda, T., Kawai, K., Nakamura, A., Kurokawa, K., Murakumo, Y., Ichihara, M. and Takahashi, M. (2004). A targeting mutation of tyrosine 1062 in Ret causes a marked decrease of enteric neurons and renal hypoplasia. *Mol. Cell. Biol.* **24**, 8026-8036.
Kim, J. H., Huang, Z. and Mo, R. (2005). Gli3 null mice display glandular overgrowth of the developing stomach. *Dev. Dyn.* **234**, 984-991.
Kolterud, A., Grosse, A. S., Zacharias, W. J., Walton, K. D., Kretovich, K. E., Madison, B. B., Waghray, M., Ferris, J. E., Hu, C., Merchant, J. L. et al. (2009). Paracrine Hedgehog signaling in stomach and intestine: new roles for hedgehog in gastrointestinal patterning. *Gastroenterology* **137**, 618-628.
Lee, C. S., Buttitta, L. and Fan, C. M. (2001a). Evidence that the WNT-inducible *growth arrest-specific gene 1* encodes an antagonist of sonic hedgehog signaling in the somite. *Proc. Natl. Acad. Sci. USA* **98**, 11347-11352.
Lee, C. S., May, N. R. and Fan, C. M. (2001b). Transdifferentiation of the ventral retinal pigmented epithelium to neural retina in the *growth arrest specific gene 1* mutant. *Dev. Biol.* **236**, 17-29.
Litingtung, Y., Lei, L., Westphal, H. and Chiang, C. (1998). Sonic hedgehog is essential to foregut development. *Nat. Genet.* **20**, 58-61.
Liu, Y., Liu, C., Yamada, Y. and Fan, C. M. (2002). *growth arrest specific gene 1* acts as a region-specific mediator of the *Fgf10/Fgf8* regulatory loop in the limb. *Development* **129**, 5289-5300.
López-Ramírez, M. A., Domínguez-Monzón, G., Vergara, P. and Segovia, J. (2008). Gas1 reduces Ret tyrosine 1062 phosphorylation and alters GDNF-mediated intracellular signaling. *Int. J. Dev. Neurosci.* **26**, 497-503.
Lu, M. and Krauss, R. S. (2010). N-cadherin ligation, but not Sonic hedgehog binding, initiates Cdo-dependent p38alpha/beta MAPK signaling in skeletal myoblasts. *Proc. Natl. Acad. Sci. USA* **107**, 4212-4217.
Madhala-Levy, D., Williams, V. C., Hughes, S. M., Reshef, R. and Halevy, O. (2012). Cooperation between Shh and IGF-I in promoting myogenic proliferation and differentiation via the MAPK/ERK and PI3K/Akt pathways requires Smo activity. *J. Cell. Physiol.* **227**, 1455-1464.
Mao, J., Kim, B. M., Rajurkar, M., Shivdasani, R. A. and McMahon, A. P. (2010). Hedgehog signaling controls mesenchymal growth in the developing mammalian digestive tract. *Development* **137**, 1721-1729.
Martinelli, D. C. and Fan, C. M. (2007a). *Gas1* extends the range of Hedgehog action by facilitating its signaling. *Genes Dev.* **21**, 1231-1243.
Martinelli, D. C. and Fan, C. M. (2007b). The role of Gas1 in embryonic development and its implications for human disease. *Cell Cycle* **6**, 2650-2655.
Mograbi, B., Bocciardi, R., Bourget, I., Busca, R., Rochet, N., Farahi-Far, D., Juhel, T. and Rossi, B. (2001). Glial cell line-derived neurotrophic factor-stimulated phosphatidylinositol 3-kinase and Akt activities exert opposing effects on the ERK pathway: importance for the rescue of neuroectodermic cells. *J. Biol. Chem.* **276**, 45307-45319.
Moore, M. W., Klein, R. D., Fariñas, I., Sauer, H., Armanini, M., Phillips, H., Reichardt, L. F., Ryan, A. M., Carver-Moore, K. and Rosenthal, A. (1996). Renal and neuronal abnormalities in mice lacking GDNF. *Nature* **382**, 76-79.
Mo, R., Kim, J. H., Zhang, J., Chiang, C., Hui, C.-C. and Kim, P. C. W. (2001). Anorectal malformations caused by defects in Sonic hedgehog signaling. *Am. J. Pathol.* **159**, 765-774.
Natarajan, D., Marcos-Gutierrez, C., Pachnis, V. and de Graaff, E. (2002). Requirement of signalling by receptor tyrosine kinase RET for the directed migration of enteric nervous system progenitor cells during mammalian embryogenesis. *Development* **129**, 5151-5160.
Newgreen, D. and Young, H. M. (2002). Enteric nervous system: development and developmental disturbances–part 1. *Pediatr. Dev. Pathol.* **5**, 224-247.
Pichel, J. G., Shen, L., Sheng, H. Z., Granholm, A. C., Drago, J., Grinberg, A., Lee, E. J., Huang, S. P., Saarma, M., Hoffer, B. J. et al. (1996). Defects in enteric innervation and kidney development in mice lacking GDNF. *Nature* **382**, 73-76.
Pineda-Alvarez, D. E., Roessler, E., Hu, P., Srivastava, K., Solomon, B. D., Siple, C. E., Fan, C. M. and Muenke, M. (2012). Missense substitutions in the GAS1 protein present in holoprosencephaly patients reduce the affinity for its ligand, SHH. *Hum. Genet.* **131**, 301-310.
Ramalho-Santos, M., Melton, D. A. and McMahon, A. P. (2000). Hedgehog signals regulate multiple aspects of gastrointestinal development. *Development* **127**, 2763-2772.
Reichenbach, B., Delalande, J. M., Kolmogorova, E., Prier, A., Nguyen, T., Smith, C. M., Holzschuh, J. and Shepherd, I. T. (2008). Endoderm-derived Sonic hedgehog and mesoderm Hand2 expression are required for enteric nervous system development in zebrafish. *Dev. Biol.* **318**, 52-64.
Riddlesberger, M. M., Jr. (1989). Congenital abnormalities of the gastrointestinal system. In *Textbook Of Gastroenterology And Nutrition In Infancy* (ed. E. Lebenthal), pp. 761-779. New York: Raven Press.
Riobo, N. A., Haines, G. M. and Emerson, C. P., Jr. (2006a). Protein kinase C-δ and mitogen-activated protein/extracellular signal-regulated kinase-1 control GLI activation in hedgehog signaling. *Cancer Res.* **66**, 839-845.
Riobó, N. A., Lu, K., Ai, X., Haines, G. M. and Emerson, C. P., Jr. (2006b). Phosphoinositide 3-kinase and Akt are essential for Sonic Hedgehog signaling. *Proc. Natl. Acad. Sci. USA* **103**, 4505-4510.
Sánchez, M. P., Silos-Santiago, I., Frisén, J., He, B., Lira, S. A. and Barbacid, M. (1996). Renal agenesis and the absence of enteric neurons in mice lacking GDNF. *Nature* **382**, 70-73.
Schaeren-Wiemers, N. and Gerfin-Moser, A. (1993). A single protocol to detect transcripts of various types and expression levels in neural tissue and cultured cells: in situ hybridization using digoxigenin-labelled cRNA probes. *Histochemistry* **100**, 431-440. .
Schneider, C., King, R. M. and Philipson, L. (1988). Genes specifically expressed at growth arrest of mammalian cells. *Cell* **54**, 787-793.
Schuchardt, A., D'Agati, V., Larsson-Blomberg, L., Costantini, F. and Pachnis, V. (1994). Defects in the kidney and enteric nervous system of mice lacking the tyrosine kinase receptor Ret. *Nature* **367**, 380-383.
Schueler-Furman, O., Glick, E., Segovia, J. and Linial, M. (2006). Is GAS1 a co-receptor for the GDNF family of ligands? *Trends Pharmacol. Sci.* **27**, 72-77.
Taraviras, S. and Pachnis, V. (1999). Development of the mammalian enteric nervous system. *Curr. Opin. Genet. Dev.* **9**, 321-327.
Taraviras, S., Marcos-Gutierrez, C. V., Durbec, P., Jani, H., Grigoriou, M., Sukumaran, M., Wang, L. C., Hynes, M., Raisman, G. and Pachnis, V. (1999). Signalling by the RET receptor tyrosine kinase and its role in the development of the mammalian enteric nervous system. *Development* **126**, 2785-2797.
Tomac, A. C., Grinberg, A., Huang, S. P., Nosrat, C., Wang, Y., Borlongan, C., Lin, S. Z., Chiang, Y. H., Olson, L., Westphal, H. et al. (1999). Glial cell line-derived neurotrophic factor receptor α1 availability regulates glial cell line-derived neurotrophic factor signaling: evidence from mice carrying one or two mutated alleles. *Neuroscience* **95**, 1011-1023.
Wegorzewska, M., Krauss, R. S. and Kang, J. S. (2003). Overexpression of the immunoglobulin superfamily members CDO and BOC enhances differentiation of the human rhabdomyosarcoma cell line RD. *Mol. Carcinog.* **37**, 1-4.
Wong, A., Bogni, S., Kotka, P., de Graaff, E., D'Agati, V., Costantini, F. and Pachnis, V. (2005). Phosphotyrosine 1062 is critical for the *in vivo* activity of the Ret9 receptor tyrosine kinase isoform. *Mol. Cell. Biol.* **25**, 9661-9673.
Worley, D. S., Pisano, J. M., Choi, E. D., Walus, L., Hession, C. A., Cate, R. L., Sanicola, M. and Birren, S. J. (2000). Developmental regulation of GDNF response and receptor expression in the enteric nervous system. *Development* **127**, 4383-4393.
Yan, H., Bergner, A. J., Enomoto, H., Milbrandt, J., Newgreen, D. F. and Young, H. M. (2004). Neural cells in the esophagus respond to glial cell line-derived neurotrophic factor and neurturin, and are RET-dependent. *Dev. Biol.* **272**, 118-133.
Yang, J. T., Liu, C. Z., Villavicencio, E. H., Yoon, J. W., Walterhouse, D. and Iannaccone, P. M. (1997). Expression of human GLI in mice results in failure to thrive, early death, and patchy Hirschsprung-like gastrointestinal dilatation. *Mol. Med.* **3**, 826-835.
Young, H. M., Hearn, C. J., Farlie, P. G., Canty, A. J., Thomas, P. Q. and Newgreen, D. F. (2001). GDNF is a chemoattractant for enteric neural cells. *Dev. Biol.* **229**, 503-516.
Zhang, X. M., Ramalho-Santos, M. and McMahon, A. P. (2001). *Smoothened* mutants reveal redundant roles for Shh and Ihh signaling including regulation of L/R symmetry by the mouse node. *Cell* **105**, 781-792.